Inorg. Chem. **2002**, *41*, 5373–5381

New Oxamato-Bridged Trinuclear Cu^{II}–Cu^{II}–Cu^{II} Complexes with Hydrogen-Bond Supramolecular Structures: Synthesis and Magneto–Structural Studies

Javier Tercero, Carmen Diaz,* and Joan Ribas

Departament de Química Inorgànica, Universitat de Barcelona, Martí i Franquès 1-11, 08028 Barcelona, Spain

José Mahía and Miguel Angel Maestro

Servicios Xerais de Apoio a Investigación, Universidad da Coruña, Campus da Zapateira, s/n 15071, A Coruña, Spain

Received October 18, 2001

Three oxamato-bridged copper(II) complexes of formula $[\{Cu(H_2O)(tmen)Cu(tmen)\}\{\mu\text{-}Cu(H_2O)(Me_2pba)\}]_n\{(PF_6)_2\}_n \cdot 2nH_2O$ (**1**), $[\{Cu(H_2O)(tmen)Cu(NCS)(tmen)\}\{\mu\text{-}Cu(H_2O)(Me_2pba)\}]_2(ClO_4)_2 \cdot 4H_2O$ (**2**), and $[\{Cu(H_2O)(tmen)Cu(NCS)(tmen)\}\{\mu\text{-}Cu(H_2O)(Me_2pba)\}]_2(PF_6)_2 \cdot 4H_2O$ (**3**), where Me_2pba = 2,2-dimethyl-1,3-propylenebis(oxamato) and tmen = *N*,*N*,*N*′,*N*′-tetramethylethylenediamine, have been synthesized and characterized. Their crystal structures were solved. Complex **1** crystallizes in the monoclinic system, space group $P2_1$, with $a = 15.8364(3)$ Å, $b = 8.4592(2)$ Å, $c = 15.952$ Å, $\beta = 101.9070(10)°$, and $Z = 2$. Complex **2** crystallizes in the monoclinic system, space group $P2_1/c$, with $a = 6.69530(10)$ Å, $b = 18.2441(3)$ Å, $c = 31.6127(5)$ Å, $\beta = 90.1230(10)°$, and $Z = 4$. Complex **3** crystallizes in the monoclinic system, space group $P2_1/c$, with $a = 6.68970(10)$ Å, $b = 18.150$ Å, $c = 32.1949(4)$ Å, $\beta = 90.0820(10)°$, and $Z = 4$. The three complexes have a central core in common: a trinuclear Cu^{II} complex with the two terminal Cu^{II} ions blocked by *N*,*N*,*N*′,*N*′-tetramethylethylenediamine. The structure of complex **1** consists of trinuclear cationic entities connected by hydrogen bonds to produce a supramolecular one-dimensional array. The structure of complexes **2** and **3** consist of trinuclear cationic entities linked by pairs by hydrogen bonds between the water molecule of the central Cu^{II} and one oxygen atom of the oxamato ligand of the neighboring entity, forming a hexanuclear complex. The magnetic properties of the three complexes were studied by susceptibility vs temperature measurement. For complexes **1**–**3** the fit was made by the irreducible tensor operator (ITO). The values obtained were $J_1 = -386.48$ cm^{-1} and $J_2 = 1.94$ cm^{-1} for **1**, $J_1 = -125.77$ cm^{-1} and $J_2 = 0.85$ cm^{-1} for **2**, and $J_1 = -135.50$ cm^{-1} and $J_2 = 0.94$ cm^{-1} for **3**. In complex **1**, the coordination polyhedron of the terminal Cu^{II} atoms can be considered as square pyramidal; the apical positions are filled by the oxygen atom from a water molecule in the former and a F atom of the hexafluorophosphate anion in the latter showing a quasi-planar $\{Cu(CuMe_2pba)Cu\}$ network. For complexes **2** and **3**, the square pyramidal environment of the terminal Cu(II) ions was strongly modified. To our knowledge, this is the first time that the longest distance (apical) in complexes with oxamato derivatives and bidentate amines as blocking ligands has been reported in one of the oxamato arms. The great difference in J_1 values between **1** and the other two complexes is interpreted as an orbital reversal of the magnetic orbitals of the terminal Cu^{II} ions in **2** and **3**.

Introduction

Research has recently focused on the ability to control the construction of coordination supramolecular arrays based on covalent interactions or hydrogen bonding for the rational design of functional materials.[1] Journaux et al.[2] have reported that the pathways used to obtain these species are mainly

* To whom correspondence should be addressed. E-mail: carme.diaz@qi.ub.es.

(1) *Supramolecular Chemistry, Concepts and Perspectives*; Lehn, J. M., Ed.; VCH: Weinheim, Germany, 1995.

10.1021/ic011081i CCC: $22.00
Published on Web 09/28/2002

Scheme 1

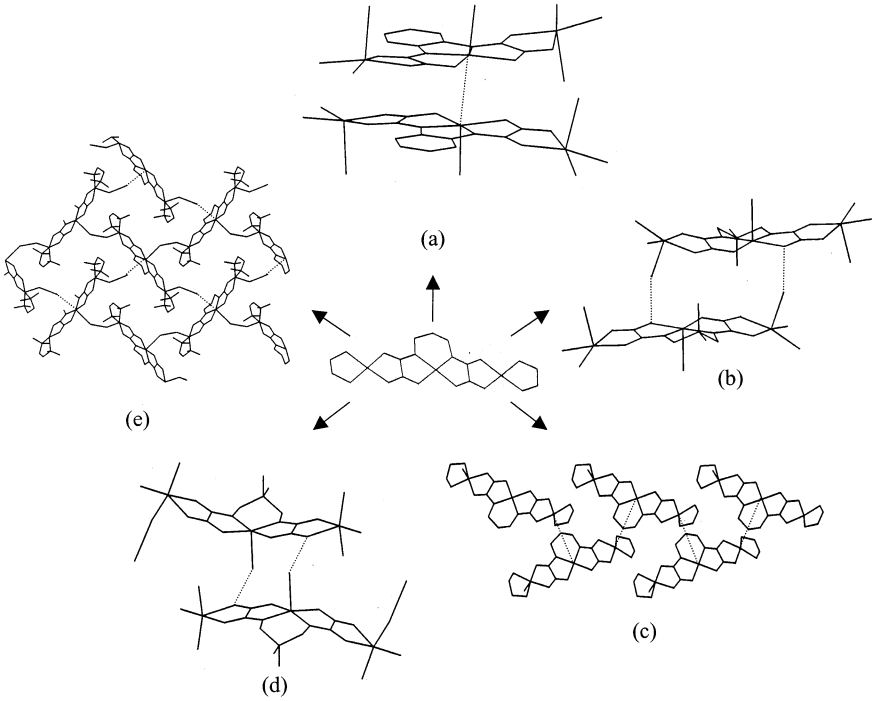

based on the following synthetic schemes: (a) the self-assembled method; (b) the use of polynucleating ligands; (c) the use of complexes as ligands. Following these principles, supramolecular architectures have been reported with oxamidates[3] and oxamates.[4] Simple mononuclear bis-(oxamato)copper(II) complexes can give supramolecular architectures.[5] Several oxamidato−Cu^{II} dinuclear complexes also give supramolecular structures, through hydrogen bonds,[6] carboxylato ligands,[7] N-donor spacers,[8] or small inorganic bridges (NO_2^-, N_3^-).[9] With oxamidato−Ni^{II}−Cu^{II} entities, tetranuclear systems with SCN^- bridging ligands,[10] one-dimensional complexes in which the heterodinuclear entities are linked by the nitrite groups,[11] and, very recently, a supramolecular structure, in which the Cu−Ni entities are linked by hydrogen bond and behave as molecule-based magnet, have been reported by the authors.[12] So far, the number of supramolecular systems derived from trinuclear Cu^{II}−Cu^{II}−Cu^{II} entities is very limited: with oxamidato ligand only one Cu_3 supramolecular structure has been reported.[13] In recent years, we have focused our aim to link in a supramolecular manner trinuclear Cu^{II} complexes derived from bis(oxamato)copper(II) systems. All reported species are schematically shown in Scheme 1.

With *o*-phenylenebis(oxamato) there is a new complex with a short distance between the central Cu^{II} ions of two separate entities (Scheme 1a),[14] with 2,2-dimethyl-1,3-propylenebis(oxamato) there are new hexanuclear systems with hydrogen bonds between a water molecule of one terminal Cu^{II} and one oxygen atom of the oxamato ligand of the neighboring entity (Scheme 1b),[14] and with 2-hydroxy-1,3-propylenebis(oxamato) there is a new one-dimensional system contributing the oxygen of the −OH group (analogous Scheme 1c).[4,14] When the oxamato was 1,3-propanediylbis(oxamato) and using XCN^- (X = S, Se) as bridging ligand, there is a new pseudo-two-dimensional system (Scheme 1e).[15] With the aim to synthesize new

(2) Aukauloo, A.; Ottenwaelder, X.; Ruiz, R.; Journaux, Y.; Pei, Y.; Rivière, E.; Muñoz, C. *Eur. J. Inorg. Chem.* **2000**, 951 and references therein.
(3) Colacio, E.; López-Magaña, C.; Mc-Kee, V.; Romerosa, A. *J. Chem. Soc., Dalton Trans.* **1999**, 2923 and references therein.
(4) Gao, E. Q.; Zhao, Q. H.; Tang, J. K.; Liao, D. Z.; Jiang, Z. H.; Yan, S. P. *J. Chem. Soc., Dalton Trans.* **2001**, 1537 and references therein.
(5) Unamuno, I.; Gutiérrez-Zorrilla, J. M.; Luque, A.; Román, P.; Lezama, L.; Calvo, R.; Rojo, T. *Inorg. Chem.* **1998**, *37*, 6452.
(6) Lloret, F.; Julve, M.; Faus, J.; Journaux, Y.; Philoche-Levisalles, M.; Jeannin, Y. *Inorg. Chem.* **1989**, *28*, 3702.
(7) (a) Chen, Z. N.; Liu, S. X.; Qiu, J.; Wang, Z. M.; Huang, J. L.; Tang, W. X. *J. Chem. Soc., Dalton Trans.* **1994**, 2989. (b) Chen, Z. N.; Tang, W. X.; Miao, F. M.; Wang, J. L. *Polyhedron* **1994**, *13*, 2543. (c) Kawata, S.; Kitagawa, S.; Machida, H.; Nakamoto, T.; Kondo, M.; Katada, M.; Kikuchi, K.; Ikemoto, I. *Inorg. Chim. Acta* **1995**, *229*, 211. (d) Zhang, H.-X.; Kang, B.-S.; Xu, A.-W.; Chen, Z.-N.; Zhou, Z.-Y.; Chan, A. S. C.; Yu, K.-B.; Ren, C. *J. Chem. Soc., Dalton Trans.* **2001**, 2559.
(8) (a) Chen, Z. N.; Qiu, J.; Tang, W. X.; Yu, K. B. *Inorg. Chim. Acta* **1994**, *224*, 171. (b) Chen, Z. N.; Fu, D. G.; Yu, K. B.; Tang, W. X. *J. Chem. Soc., Dalton Trans.* **1994**, 1917. (c) Domínguez-Vera, J. M.; Moreno, J. M.; Gálvez, N.; Suarez-Varela, J.; Colacio, E.; Kivekas, R.; Klinga, M. *Inorg. Chim. Acta* **1998**, *281*, 95. (d) Zhang, H.-W.; Kang, B.-S.; Zhou, Z.-Y.; Chan, A. S. C.; Chen, Z.-N.; Ren, C. *J. Chem. Soc., Dalton Trans.* **2001**, 1664.
(9) (a) Real, J. A.; Ruiz, R.; Faus, J.; Lloret, F.; Julve, M.; Journaux, Y.; Philoche-Levisalles, M.; Bois, C. *J. Chem. Soc., Dalton Trans.* **1994**, 3769. (b) Chen, Z. N.; Qiu, J.; Wu, Z. W.; Fu, D. G.; Yu, K. B.; Tang, W. X. *J. Chem. Soc., Dalton Trans.* **1994**, 1923. (c) Costes, J.-P.; Dahan, F.; Laurent, J.-P.; Drillon, M. *Inorg. Chim. Acta* **1999**, *294*, 8.
(10) Ribas, J.; Diaz, C.; Costa, R.; Tercero, J.; Solans, X.; Font-Bardía, M.; Stoeckli-Evans, H. *Inorg. Chem.* **1998**, *37*, 233.
(11) Diaz, C.; Ribas, J.; Costa, R.; Tercero, J.; El Fallah, M. S.; Solans, X.; Font-Bardía, M. *Eur. J. Inorg. Chem.* **2000**, 675.
(12) Tercero, J.; Diaz, C.; Ribas, J.; Mahía, J.; Maestro, M. *Chem. Commun.* **2002**, 364.
(13) Journaux, Y.; Sletten, J.; Kahn, O. *Inorg. Chem.* **1986**, *25*, 439.
(14) Tercero, J.; Diaz, C.; El Fallah, M. S.; Ribas, J.; Maestro, M. A.; Mahía, J. *Inorg Chem.* **2001**, *40*, 3077.
(15) (a) Ribas, J.; Diaz, C.; Solans, X.; Font-Bardía, M. *Inorg. Chim. Acta* **1995**, *231*, 229. (b) Ribas, J.; Diaz, C.; Solans, X.; Font-Bardía, M. *J. Chem. Soc., Dalton Trans.* **1997**, 35.

systems to find possible magnetic ordering, here we report two new supramolecular systems, linking trinuclear Cu^{II} entities by hydrogen bonds: a one-dimensional array in $[\{Cu(H_2O)(tmen)Cu(tmen)\}\{\mu\text{-}Cu(H_2O)(Me_2pba)\}]_n\{(PF_6)_2\}_n \cdot 2nH_2O$ (**1**), in which the trinuclear entities are linked through hydrogen bonds from the oxygen atoms of the apical water molecules from terminal and central Cu^{II} ions (Scheme 1c), and two hexanuclear complexes $[\{Cu(H_2O)(tmen)Cu(NCS)(tmen)\}\{\mu\text{-}Cu(H_2O)(Me_2pba)\}]_2(ClO_4)_2 \cdot 4H_2O$ (**2**) and $[\{Cu(H_2O)(tmen)Cu(NCS)(tmen)\}\{\mu\text{-}Cu(H_2O)(Me_2pba)\}]_2(PF_6)_2 \cdot 4H_2O$ (**3**), in which the trinuclear entities are linked by hydrogen bonds between the water molecule of the central Cu^{II} and one oxygen atom of the oxamato ligand of the neighboring entity and the SCN^- behaves as terminal ligand (Scheme 1d).

Magnetic properties of these three new supramolecular systems have been studied. The magnetic coupling through the oxamato(2−) ligand is strongly antiferromagnetic, owing to the broad overlap between the magnetic orbital of the three metal ions through the corresponding molecular orbital of the oxamato bridge.[16] As indicated above, we mainly focused on the association of the "molecular spins" (trinuclear entities) that take place when the supramolecular assemblies are formed. No long-range magnetic ordering has been found. With these supramolecular systems, long-range magnetic order has been only reported for a discrete dinuclear system,[12] as commented above, and for some systems starting from one-dimensional or two-dimensional precursors, fully interlocked.[17]

Experimental Section

Caution! Perchlorate complexes of metal ions are potentially explosive. Only a small amount of material should be prepared, and this should be handled with caution.

Synthesis of the New Complexes. The copper(II) precursor, $Na_2[Cu(Me_2pba)] \cdot 3H_2O$, was prepared as described elsewhere.[14]

$[\{Cu(H_2O)(tmen)Cu(tmen)\}\{\mu\text{-}Cu(H_2O)(Me_2pba)\}]_n\{(PF_6)_2\}_n \cdot 2nH_2O$ (1). An ethanolic solution (15 mL) of tmen (0.313 g, 2.69 mmol) was added to an ethanolic solution (15 mL) of $Cu(ClO_4)_2 \cdot 6H_2O$ (0.650 g, 2.69 mmol). To this mixture, an aqueous solution (50 mL) of $Na_2[Cu(Me_2pba)] \cdot 3H_2O$ (0.547 g, 1.36 mmol) and an aqueous solution (10 mL) of NH_4PF_6 (0.219 g, 1.36 mmol) were added successively. After filtration to remove any impurities, the solution was left undisturbed, and well-formed blue-green crystals were obtained after several days. The yield was ca. 70%. Anal. Calcd for $C_{21}H_{48}Cu_3F_{12}N_6O_9P_2$ (M_r = 1009.21): C, 25.0; H, 4.79; N, 8.33. Found: C, 24.7; H, 4.7; N, 8.4.

$[\{Cu(H_2O)(tmen)Cu(NCS)(tmen)\}\{\mu\text{-}Cu(H_2O)(Me_2pba)\}]_2(ClO_4)_2 \cdot 4H_2O$ (2). To an aqueous solution (50 mL) of $[\{Cu(H_2O)(tmen)\}_2\{\mu\text{-}Cu(H_2O)(Me_2pba)\}]_2\{(ClO_4)_2\}_2$ previously reported by us[14] (1.25 g, 1.36 mmol) was added an aqueous solution (10 mL) of NH_4SCN (0.103 g, 1.36 mmol) with constant stirring. The resultant solution was filtered to remove any impurity and left to evaporate slowly at room temperature. Dark blue monocrystals suitable for X-ray determination were collected after 2 weeks. The yield was ca. 80%. Anal. Calcd for $C_{22}H_{50}ClCu_3N_7O_{14}S$ (M_r = 894.82): C, 29.53; H, 5.63; N, 10.96; S, 3.58. Found: C, 29.7; H, 5.4; N, 11.1; S, 3.4.

$[\{Cu(H_2O)(tmen)Cu(NCS)(tmen)\}\{\mu\text{-}Cu(H_2O)(Me_2pba)\}]_2(PF_6)_2 \cdot 4H_2O$ (3). To an aqueous solution (50 mL) of complex **1** (1.37 g, 1.36 mmol) was added an aqueous solution (10 mL) of NH_4SCN (0.103 g, 1.36 mmol) with constant stirring. The resultant solution was filtered to remove any impurity and left to evaporate slowly at room temperature. Dark blue monocrystals suitable for X-ray determination were collected after 3 weeks. The yield was ca. 65%. Anal. Calcd for $C_{22}H_{50}Cu_3F_6N_7O_{10}PS$ (M_r = 940.34): C, 28.10; H, 5.27; N, 10.43; S, 3.41. Found: C, 27.9; H, 5.4; N, 10.2; S, 3.5.

Crystal Structure Determination. Suitable crystals of **1** (block, blue, dimensions 0.30 × 0.25 × 0.20 mm), **2** (needle, blue, dimensions 0.55 × 0.05 × 0.05 mm), and **3** (needle, blue, dimensions 0.50 × 0.07 × 0.05 mm) were used for the structure determination. X-ray data were collected using a Bruker SMART CCD area detector single-crystal diffractometer with graphite-monochromatized Mo Kα radiation (λ = 0.710 73 Å) by the $\phi-\omega$ scan method at room temperature. A total of 1271 frames of intensity data were collected for each compound. The first 50 frames were recollected at the end of data collection to monitor for decay. In each case, the crystals used for the diffraction studies showed no decomposition during data collection. The integration process yielded a total of 14 419 reflections for **1**, 25 882 for **2,** and 26 496 for **3**, of which 9499 [R(int) = 0.0255], 9435 [R(int) = 0.0511], and 9571 [R(int) = 0.0532], respectively, were independent. Absorption corrections were applied using the SADABS[18] program (maximum and minimum transmission coefficients, 0.729 and 0.631 for **1**, 1.000 and 0.811 for **2**, and 0.916 and 0.467 for **3**). The structures were solved using the Bruker SHELXTL-PC[19] software by direct methods and refined by full-matrix least-squares methods on F^2. Hydrogen atoms were included in calculated positions and refined in the riding mode, except those of water molecules that were located on residual density maps, but their positions were then fixed and refined in the riding mode. Hydrogen atoms of water molecules for **3** were not included. For **1** convergence was reached at a final R1 = 0.0662 [for $I > 2\sigma(I)$], wR2 = 0.2058 (for all data), and 488 parameters, with allowance for the thermal anisotropy for all non-hydrogen atoms. The weighting scheme employed was $w = [\sigma^2(F_o^2 + (0.1193\,P)^2 + 0.8371P]$ and $P = (|F_o|^2+2|F_c|^2)/3$, and the goodness of fit on F^2 was 1.018 for all observed reflections. For **2**, convergence was reached at a final R1 = 0.0572 [for $I > 2\sigma(I)$], wR2 = 0.1578 (for all data), and 465 parameters, with allowance for the thermal anisotropy for all non-hydrogen atoms. The weighting scheme employed was $w = [\sigma^2(F_o^2 + (0.0712P)^2 + 0.3440P]$ and $P = (|F_o|^2 + 2|F_c|^2)/3$, and the goodness of fit on F^2 was 1.092 for all observed reflections. For **3**, convergence was reached at a final R1 = 0.0697 [for $I > 2\sigma(I)$], wR2 = 0.1892 (for all data), and 461 parameters, with allowance for the thermal anisotropy for all non-hydrogen atoms. The weighting scheme employed was $w = [\sigma^2(F_o^2 + (0.0761P)^2 + 5.9930P]$ and $P = (|F_o|^2 + 2|F_c|^2)/3$, and the goodness of fit on F^2 was 1.077 for all observed reflections. The perchlorate and hexafluorophosphate

(16) (a) Costa, R.; Garcia, A.; Ribas, J.; Mallah, T.; Journaux, Y.; Sletten, J.; Solans, X.; Rodríguez, V. *Inorg. Chem.* **1993**, *32*, 3733. (b) Hay, P. J.; Thibeault, J. C.; Hoffmann, R. *J. Am. Chem. Soc.* **1975**, *97*, 4884.

(17) (a) Stumpf, H. O.; Ouahab, L.; Pei, Y.; Bergerat, P.; Kahn, O. *J. Am. Chem. Soc.* **1994**, *116*, 3866. (b) Vaz, M. G. F.; Pinheiro, L. M. M.; Stumpf, H. O.; Alcantara, A. F. C.; Golhen, S.; Ouahab, L.; Cador, O.; Mathonière, C.; Kahn, O. *Chem.—Eur. J.* **1999**, *5*, 1486 and references therein.

(18) Sheldrick, G. M. *SADABS*; University of Göttingen: Göttingen, Germany, 1996. Program for absorption corrections using Bruker CCD data.

(19) Sheldrick, G. M. *Bruker SHELXTL-PC*; University of Göttingen: Göttingen, Germany, 1997.

Table 1. Crystallographic Data for Complexes **1**−**3**

param	**1**	**2**	**3**
empirical formula	$C_{21}H_{48}Cu_3F_{12}N_6O_9P_2$	$C_{22}H_{50}ClCu_3N_7O_{14}S$	$C_{22}H_{50}Cu_3F_6N_7O_{10}PS$
fw	1009.21	894.82	940.34
space group	$P2_1$	$P2_1/c$	$P2_1/c$
Z	2	4	4
a (Å)	15.836(1)	6.695(1)	6.690(1)
b (Å)	8.459(1)	18.244(1)	18.150(1)
c (Å)	15.952(1)	31.613(1)	32.195(1)
β (deg)	101.907(1)	90.123(1)	90.082(1)
V (Å^3)	2091.0(1)	3861.5(1)	3909.15(8)
ρ_{calc} (g/cm^3)	1.603	1.539	1.598
μ_{calc} (mm^{-1})	1.689	1.826	1.794
λ(Mo Kα), Å	0.710 73	0.710 73	0.710 73
temp (K)	298(2)	298(2)	298(2)
final R indices[a]	R1 = 0.0662	R1 = 0.0572	R1 = 0.0697
($I > 2\sigma(I)$]	wR2 = 0.1731	wR2 = 0.1285	wR2 = 0.1542
final R indices	R1 = 0.1009	R1 = 0.1155	R1 = 0.1315
(for all data)	wR2 = 0.2058	wR2 = 0.1578	wR2 = 0.1892

[a] $R1 = \sum||F_o| - |F_c||/\sum|F_o|$. [b] $wR2 = \{\sum(w(F_o^2 - F_c^2)^2]/\sum(w(F_o^2)^2]\}^{1/2}$.

Table 2. Selected Bond Lengths (Å) and Angles (deg) for **1**

Cu(1)−O(1)	1.945(5)	Cu(2)−O(3)	1.975(5)
Cu(1)−O(2)	2.010(5)	Cu(2)−O(4)	1.988(6)
Cu(1)−N(1)	2.016(7)	Cu(2)−O(2S)	2.450(8)
Cu(1)−N(2)	2.027(7)	Cu(3)−O(5)	1.925(6)
Cu(1)−O(1S)	2.275(7)	Cu(3)−O(6)	1.959(5)
Cu(2)−N(3)	1.932(6)	Cu(3)−N(5)	2.002(7)
Cu(2)−N(4)	1.955(6)	Cu(3)−N(6)	2.009(6)
O(1)−Cu(1)−O(2)	84.2(2)	N(3)−Cu(2)−O(4)	176.5(3)
O(1)−Cu(1)−N(1)	170.4(3)	N(4)−Cu(2)−O(4)	84.8(2)
O(2)−Cu(1)−N(1)	93.0(2)	O(3)−Cu(2)−O(4)	95.5(2)
O(1)−Cu(1)−N(2)	92.1(3)	N(3)−Cu(2)−O(2S)	98.0(3)
O(2)−Cu(1)−N(2)	165.8(3)	N(4)−Cu(2)−O(2S)	102.4(3)
N(1)−Cu(1)−N(2)	88.4(3)	O(3)−Cu(2)−O(2S)	82.0(3)
O(1)−Cu(1)−O(1S)	90.6(3)	O(4)−Cu(2)−O(2S)	85.4(3)
O(2)−Cu(1)−O(1S)	89.9(3)	O(5)−Cu(3)−O(6)	85.4(2)
N(1)−Cu(1)−O(1S)	98.5(3)	O(5)−Cu(3)−N(5)	94.4(2)
N(2)−Cu(1)−O(1S)	103.8(3)	O(6)−Cu(3)−N(5)	174.8(3)
N(3)−Cu(2)−N(4)	95.3(3)	O(5)−Cu(3)−N(6)	178.1(2)
N(3)−Cu(2)−O(3)	84.1(2)	O(6)−Cu(3)−N(6)	92.7(2)
N(4)−Cu(2)−O(3)	175.6(3)	N(5)−Cu(3)−N(6)	87.5(3)

Table 3. Selected Bond Lengths (Å) and Angles (deg) for **2**

Cu(1)−N(7)	1.948(4)	Cu(2)−O(1S)	2.313(3)
Cu(1)−O(1)	1.988(3)	Cu(3)−O(5)	1.965(3)
Cu(1)−N(1)	2.031(4)	Cu(3)−O(2S)	1.991(4)
Cu(1)−N(2)	2.050(4)	Cu(3)−N(6)	2.020(5)
Cu(1)−O(2)	2.288(3)	Cu(3)−N(5)	2.031(5)
Cu(2)−N(3)	1.933(3)	Cu(3)−O(6)	2.256(3)
Cu(2)−N(4)	1.941(3)	N(7)−C(22)	1.145(6)
Cu(2)−O(4)	1.982(3)	S(1)−C(22)	1.625(6)
Cu(2)−O(3)	1.986(3)		
N(7)−Cu(1)−O(1)	91.79(17)	N(3)−Cu(2)−O(1S)	106.78(14)
N(7)−Cu(1)−N(1)	92.9(2)	N(4)−Cu(2)−O(1S)	96.99(13)
O(1)−Cu(1)−N(1)	175.25(16)	O(4)−Cu(2)−O(1S)	88.75(12)
N(7)−Cu(1)−N(2)	161.8(2)	O(3)−Cu(2)−O(1S)	97.22(12)
O(1)−Cu(1)−N(2)	89.72(15)	O(5)−Cu(3)−O(2S)	85.02(15)
N(1)−Cu(1)−N(2)	85.60(17)	O(5)−Cu(3)−N(6)	178.33(19)
N(7)−Cu(1)−O(2)	95.59(18)	O(2S)−Cu(3)−N(6)	96.0(2)
O(1)−Cu(1)−O(2)	79.30(11)	O(5)−Cu(3)−N(5)	92.33(18)
N(1)−Cu(1)−O(2)	100.94(15)	O(2S)−Cu(3)−N(5)	158.1(2)
N(2)−Cu(1)−O(2)	102.48(15)	N(6)−Cu(3)−N(5)	87.2(2)
N(3)−Cu(2)−N(4)	95.26(14)	O(5)−Cu(3)−O(6)	80.35(11)
N(3)−Cu(2)−O(4)	164.41(14)	O(2S)−Cu(3)−O(6)	3.88(14)
N(4)−Cu(2)−O(4)	83.85(13)	N(6)−Cu(3)−O(6)	98.24(17)
N(3)−Cu(2)−O(3)	84.25(13)	N(5)−Cu(3)−O(6)	107.15(16)
N(4)−Cu(2)−O(3)	165.29(14)	C(22)−N(7)−Cu(1)	169.7(5)
O(4)−Cu(2)−O(3)	92.67(12)	N(7)−C(22)−S(1)	178.7(5)

anions and the crystallization water molecules showed high thermal parameters and less than ideal geometry. Crystal data and details on the data collection and refinement are summarized in Table 1.

Physical Measurements. Magnetic measurements were carried out in the "Servei de Magnetoquímica (Universitat de Barcelona)" on polycrystalline samples (ca. 20 mg) with a Quantum Design MPMS SQUID susceptometer operating at a magnetic field of 0.1 T between 2 and 300 K. The diamagnetic corrections were evaluated from Pascal's constants. EPR spectra were recorded on powder samples at X-band frequency with a Bruker 300E automatic spectrometer, varying the temperature between 4 and 298 K.

Results

Description of the Structures [{Cu(H$_2$O)(tmen)Cu(tmen)}{μ-Cu(H$_2$O)(Me$_2$pba)}]$_n${(PF$_6$)$_2$}$_n$·2nH$_2$O (1), [{Cu(H$_2$O)(tmen)Cu(NCS)(tmen)}{μ-Cu(H$_2$O)(Me$_2$pba)}]$_2$(ClO$_4$)$_2$·4H$_2$O (2), and [{Cu(H$_2$O)(tmen)Cu(NCS)(tmen)}{μ-Cu(H$_2$O)(Me$_2$pba)}]$_2$(PF$_6$)$_2$·4H$_2$O (3). Crystallographic data are found in Tables 2−4. The structure of complex **1** consists of a one-dimensional system formed by trinuclear copper(II) cations, [{Cu(H$_2$O)(tmen)Cu(tmen)}{μ-Cu(H$_2$O)(Me$_2$pba)}]$^{2+}$, hexafluorophosphate anions, and crystallization water molecules. Figures 1 and 2 show the cationic part with atom labeling scheme and a view of the packing, respectively. Within each trinuclear fragment, the terminal Cu(1) and Cu(3) atoms are (4 + 1)-coordinated. Two amino nitrogen atoms from the tmen ligand and two oxygen atoms from the oxamato form their basal planes. The apical positions are filled by the oxygen atom O(1S) from the water molecule (2.275 Å) in the former and the F(6) atom from the weakly bound hexafluorophosphate anion (2.676 Å) in the latter. The coordination polyhedron of Cu(1) can be considered a square-pyramid with a τ factor value of 0.08 (τ = 0 for a square pyramid and τ = 1 for a trigonal bipyramid),[20] whereas the Cu(3) atom is quasi square planar. The central Cu(2) atom has a (4 + 1) environment, with an equatorial plane occupied by two oxygen atoms and two nitrogen atoms from the oxamato groups. The fifth axial position is occupied by the water oxygen atom O(2S) (2.450 Å). Their coordination polyhedron can be regarded as a square pyramid with a τ factor value of 0.01. The metal

(20) Addison, A. W.; Rao, T. N.; Reedijk, J.; Rijn, J. V.; Verschoor, G. C. *J. Chem. Soc., Dalton Trans.* **1984**, 1349.

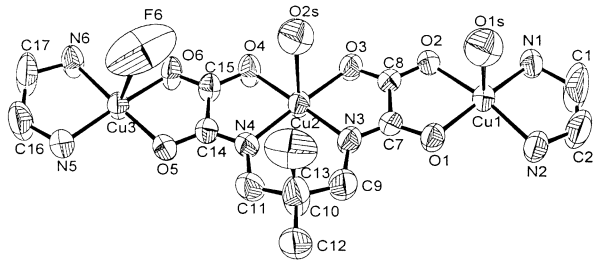

Figure 1. Drawing of the cationic part of ({Cu(H_2O)(tmen)Cu(tmen)}-{μ-Cu(H_2O)(Me_2pba)}]$_n${$(PF_6)_2$}$_n$·2nH_2O (**1**) with the atom labeling scheme. Ellipsoids are at the 50% probability level. The methyl groups of the tmen ligand have been omitted for clarity.

Table 4. Selected Bond Lengths (Å) and Angles (deg) for **3**

Cu(1)−N(7)	1.955(6)	Cu(2)−O(1S)	2.332(4)
Cu(1)−O(1)	1.983(4)	Cu(3)−O(5)	1.960(4)
Cu(1)−N(1)	2.029(5)	Cu(3)−N(5)	2.005(6)
Cu(1)−N(2)	2.062(6)	Cu(3)−N(6)	2.012(6)
Cu(1)−O(2)	2.279(4)	Cu(3)−O(2S)	2.014(5)
Cu(2)−N(4)	1.933(4)	Cu(3)−O(6)	2.264(4)
Cu(2)−N(3)	1.936(4)	N(7)−C(22)	1.139(8)
Cu(2)−O(4)	1.974(3)	S(1)−C(22)	1.610(8)
Cu(2)−O(3)	1.983(3)		
N(7)−Cu(1)−O(1)	90.6(2)	N(4)−Cu(2)−O(1S)	99.04(17)
N(7)−Cu(1)−N(1)	92.7(3)	N(3)−Cu(2)−O(1S)	104.26(16)
O(1)−Cu(1)−N(1)	176.7(2)	O(4)−Cu(2)−O(1S)	88.57(15)
N(7)−Cu(1)−N(2)	161.9(3)	O(3)−Cu(2)−O(1S)	94.45(15)
O(1)−Cu(1)−N(2)	90.57(19)	O(5)−Cu(3)−N(5)	92.8(2)
N(1)−Cu(1)−N(2)	86.1(2)	O(5)−Cu(3)−N(6)	179.2(3)
N(7)−Cu(1)−O(2)	98.1(2)	N(5)−Cu(3)−N(6)	87.9(3)
O(1)−Cu(1)−O(2)	79.20(13)	O(5)−Cu(3)−O(2S)	84.27(19)
N(1)−Cu(1)−O(2)	100.87(18)	N(5)−Cu(3)−O(2S)	158.8(3)
N(2)−Cu(1)−O(2)	99.84(19)	N(6)−Cu(3)−O(2S)	95.0(3)
N(4)−Cu(2)−N(3)	95.24(17)	O(5)−Cu(3)−O(6)	80.06(14)
N(4)−Cu(2)−O(4)	84.27(16)	N(5)−Cu(3)−O(6)	105.1(2)
N(3)−Cu(2)−O(4)	167.05(17)	N(6)−Cu(3)−O(6)	100.1(2)
N(4)−Cu(2)−O(3)	166.17(18)	O(2S)−Cu(3)−O(6)	95.06(19)
N(3)−Cu(2)−O(3)	84.34(16)	C(22)−N(7)−Cu(1)	165.8(6)
O(4)−Cu(2)−O(3)	93.04(15)	N(7)−C(22)−S(1)	177.8(7)

atoms Cu(1) and Cu(2) are displaced from the least-squares basal plane toward the apical water molecule by −0.204 and −0.068 Å, respectively. The Cu(1)−Cu(2)−Cu(3) angle is 177.082°. In the crystal (Figure 2), the neighboring trinuclear entities are linked through hydrogen bonds from the oxygen atoms O(1S) and O(2S) from the apical water molecules from Cu(1) and Cu(2), respectively, thus leading to a chain along the *c* axis. In the chain, the distances between O(2S)−H(1SA) and O(1S)−H(2SA) are 2.42 and 2.43 Å, respectively. The intramolecular metal−metal separations Cu(1)···Cu(2) and Cu(2)···Cu(3) are 5.182 and 5.132 Å, respectively, whereas the intermolecular one Cu(1)···Cu(2) is 6.202 Å. Complexes **2** and **3** are similar in structure, which consists of an hexameric system of trinuclear copper(II) cations [{Cu(H_2O)(tmen)Cu(NCS)(tmen)}{μ-Cu(H_2O)-(Me_2pba)}]$^+$, perchlorate anions for **2** and hexafluorophosphate anions for **3,** and crystallization water molecules. Figure 3 shows the common cationic part with atom labeling scheme. In complexes **2** and **3**, within each trinuclear fragment, the terminal Cu(1) and Cu(3) atoms are (4 + 1)-coordinated. For the Cu(1) ion the basal plane is formed by the two amino nitrogen atoms from the tmen ligand, an oxygen atom O(1) from the oxamato, and the nitrogen atom N(7) from the coordinated thiocyanate group. As for Cu(3), the

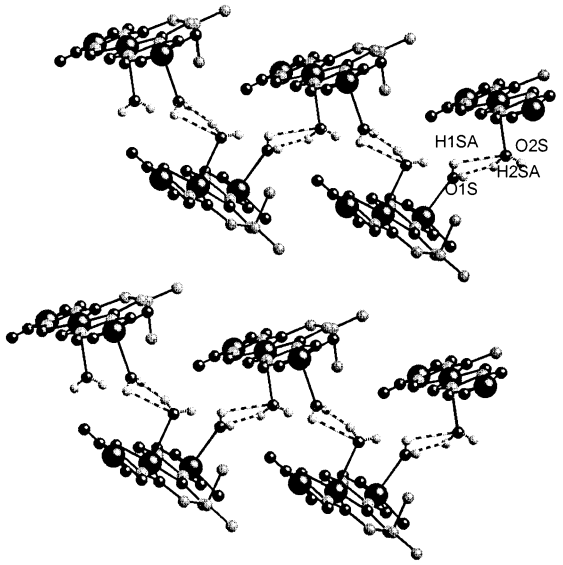

Figure 2. Projection down the *bc*-plane of the packing of ({Cu(H_2O)-(tmen)Cu(tmen)}{μ-Cu(H_2O)(Me_2pba)}]$_n${$(PF_6)_2$}$_n$·2nH_2O (**1**), showing the best view of the one-dimensional entities. The hexafluorophosphate anions are omitted for clarity.

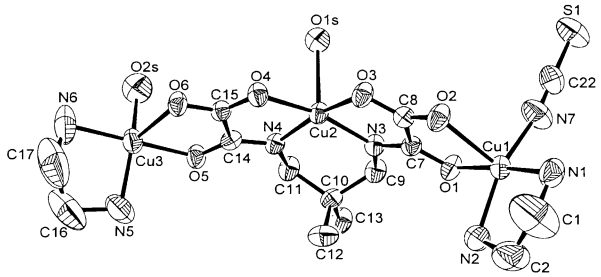

Figure 3. Drawing of the common cationic part of ({Cu(H_2O)(tmen)Cu-(NCS)(tmen)}{μ-Cu(H_2O)(Me_2pba)}]$_2$(ClO_4)$_2$·4H_2O (**2**) and ({Cu(H_2O)-(tmen)Cu(NCS)(tmen)}{μ-Cu(H_2O)(Me_2pba)}]$_2$(PF_6)$_2$·4H_2O (**3**) with the atom labeling scheme. Ellipsoids are at the 50% probability level. The methyl groups of the tmen ligand have been omitted for clarity.

basal plane consists of the two amino nitrogen atoms from the tmen ligand, an oxygen atom O(5) from the oxamato, and one oxygen atom O(2S) from the coordinated water molecule. The apical positions are filled by the oxygen atom O(2) (2.288 Å for **2** and 2.270 Å for **3**) for Cu(1) and by the oxygen O(6) (2.256 Å for **2** and 2.264 for **3**) for Cu(3), with both oxygen atoms from the oxamato ligand. The central Cu(2) atom has a (4 + 1) environment, with an equatorial plane occupied by two oxygen atoms and two nitrogen atoms from the oxamato groups. The fifth axial position is occupied by the water oxygen atom O(1S) (2.313 Å for **2** and 2.332 Å for **3**). The coordination polyhedron for Cu^{II} ions can be considered square pyramid with a τ factor value of 0.22 for Cu(1), 0.01 for Cu(2), and 0.34 for Cu(3) for complex **2** and 0.24 for Cu(1), 0.01 for Cu(2), and 0.34 for Cu(3) for complex **3**. The metal atoms Cu(1), Cu(2), and Cu(3) are displaced from the least-squares basal plane toward the apical ligand by −0.157, 0.257, and 0.176 Å for complex **2** and by −0.157, −0.227, and 0.185 Å for complex **3**. As shown in Figure 4 for **2** and **3**, two of the trinuclear entities are self-assembled by hydrogen bonds between a water molecule O(1S) of the central Cu^{II} ion and one oxygen atom of the oxamato ligand of the neighboring entity. The unit cells are

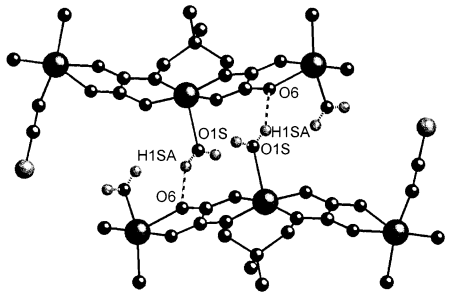

Figure 4. Drawing of the common hexanuclear entity of ({Cu(H_2O)(tmen)-Cu(NCS)(tmen)}{μ-Cu(H_2O)(Me_2pba)}]$_2$(ClO_4)$_2$·4H_2O (**2**) and ({Cu(H_2O)-(tmen)Cu(NCS)(tmen)}{μ-Cu(H_2O)(Me_2pba)}]$_2$(PF_6)$_2$·4H_2O (**3**).

shown in Figure 5a for **2** and Figure 5b for **3**. In the hexanuclear entities, the distance between O(6)−H(1SA) is 2.12 Å for **2**. Regarding complex **3**, the hydrogen atoms of the water molecules were not included and the contact distance between O(1S)−O(6) is 2.785 Å. The Cu(1)−Cu(2)−Cu(3) angles are 152.920° for **2** and 160.521° for **3**. The intramolecular metal−metal separations Cu(1)···Cu(2), Cu(2)···Cu(3) are 5.348, 5.337 Å for **2** and 5.345, 5.320 Å for **3**. The shortest intermolecular Cu···Cu distances, via the hydrogen bonds, are Cu(2)−Cu(2) = 6.152 Å and Cu(2)−Cu(3) = 6.114 Å for **2** and Cu(2)−Cu(2) = 6.113 Å and Cu(2)−Cu(3) = 6.138 Å for **3**.

Magnetic Properties. A plot of $\chi_M T$ vs temperature in a field of 0.1 T for complex **1** is shown in Figure 6. χ_M is the susceptibility/Cu_{12} unit (Figure 7; see below). The $\chi_M T$ value decreases gradually from 2.36 cm^3 mol^{-1} K between 300 and ca. 125 K (1.72 cm^3 mol^{-1} K). Between 125 and 25 K there is a plateau ($\chi_M T$ between 1.72 and 1.69 cm^3 mol^{-1} K), and from 25 to 2 K, $\chi_M T$ clearly decreases to 1.49 cm^3 mol^{-1} K. The shape of the curve from room temperature to 25 K is typical of an antiferromagnetic trinuclear Cu^{II} complex.[16a] The reduction of the $\chi_M T$ value in the low-temperature region is indicative of intermolecular interactions through hydrogen bonds which are shown in the structural part (Figure 2). To fit the experimental data (taking into account the low-temperature zone) we have assumed a ring of 12 copper(II) atoms, which should describe the behavior of the infinite chain with negligible uncertainty (Figure 7). The experimental data were fitted according to the following Hamiltonian:

$$H = -J_1(S_1S_2 + S_2S_3 + S_4S_5 + S_5S_6 + S_7S_8 + S_8S_9 + S_{10}S_{11} + S_{11}S_{12}) - J_2(S_3S_5 + S_6S_8 + S_9S_{11} + S_{12}S_2)$$

where J_1 correspond to the coupling through the oxamato bridge and J_2 to the coupling through the hydrogen bonding between trinuclear entities. The free parameters were J_1, J_2, and g (average). The fit made by the irreducible tensor operator formalism (ITO) using the CLUMAG program[21] gave the following results: $J_1 = -386.48$ cm^{-1}; $J_2 = 1.94$ cm^{-1}; $g = 2.14$; $R = 2.52 \times 10^{-5}$. As expected, with this small J_2 value, the variation of $\chi_M T$ vs T is observed only at low temperatures. The simulation of the two possible cases (ferro- and/or antiferromagnetic intermolecular interactions

(21) Gatteschi, D.; Pardi, L. *Gazz. Chim. Ital.* **1993**, *123*, 231.

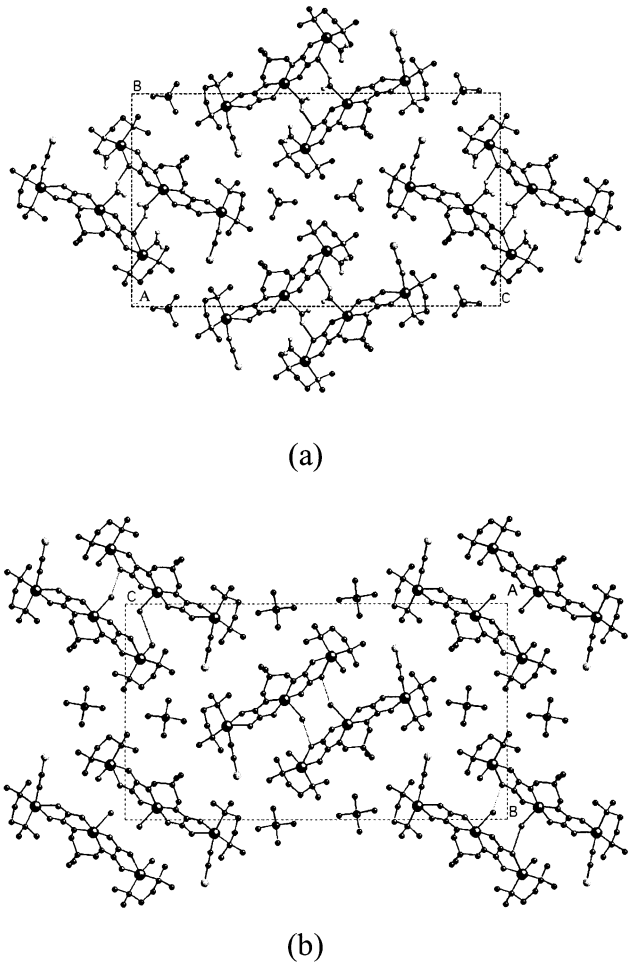

Figure 5. Projections down the *bc*-plane of the unit cells of (a) ({Cu-(H_2O)(tmen)Cu(NCS)(tmen)}{μ-Cu(H_2O)(Me_2pba)}]$_2$(ClO_4)$_2$·4H_2O (**2**) and (b) ({Cu(H_2O)(tmen)Cu(NCS)(tmen)}{μ-Cu(H_2O)(Me_2pba)}]$_2$(PF_6)$_2$·4H_2O (**3**).

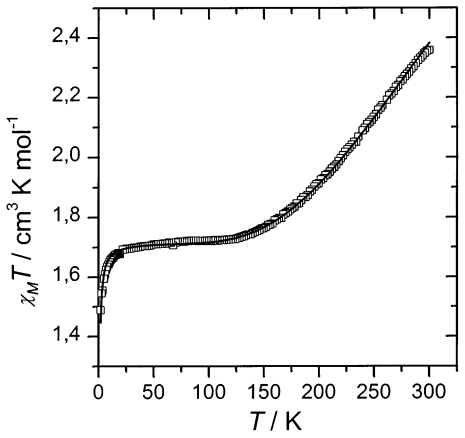

Figure 6. Experimental and calculated variations of the product $\chi_M T$ versus temperature for ({Cu(H_2O)(tmen)Cu(tmen)}{μ-Cu(H_2O)(Me_2pba)}]$_n${(PF_6)$_2$}$_n$·2$n$$H_2O$ (**1**).

for a ring of 12 atoms) has been described elsewhere.[14] When the magnetic interaction between the trinuclear entities is weakly ferromagnetic, the resulting S_T values tend to zero at low temperatures, and so the $\chi_M T$ curve decreases and tends to zero at these temperatures.

Plots of $\chi_M T$ vs temperature in a field of 0.1 T for complexes **2** and **3** are shown in Figures 8 and 9, respec-

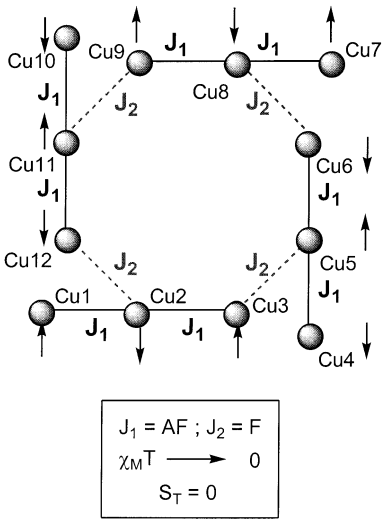

Figure 7. Scheme of the spin topology assuming intermolecular ferromagnetic coupling for a ring of 12 copper(II) atoms.

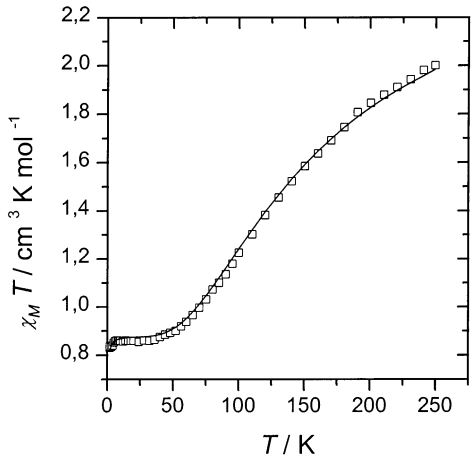

Figure 8. Experimental and calculated variations of the product $\chi_M T$ versus temperature for ({Cu(H_2O)(tmen)Cu(NCS)(tmen)}{μ-Cu(H_2O)(Me_2pba)}]$_2$-(ClO_4)$_2$·4H_2O (**2**).

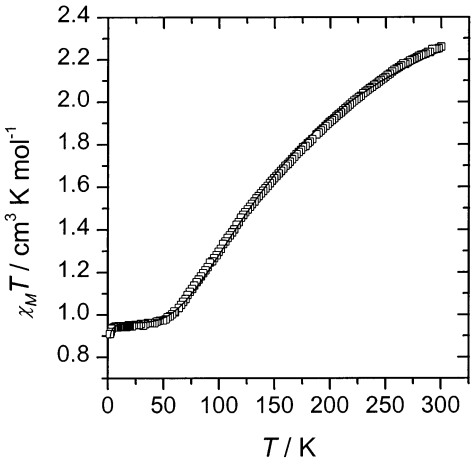

Figure 9. Experimental and calculated variations of the product $\chi_M T$ versus temperature for ({Cu(H_2O)(tmen)Cu(NCS)(tmen)}{μ-Cu(H_2O)(Me_2pba)}]$_2$-(PF_6)$_2$·4H_2O (**3**).

tively. In both cases, χ_M is the susceptibility/Cu_6 unit (Figure 10; see below). For complex **2**, the $\chi_M T$ value decreases gradually from 2.00 cm^3 mol^{-1} K at 250 K, with a plateau between 40 and 15 K (0.87 cm^3 mol^{-1} K), to 0.82 cm^3 mol^{-1}

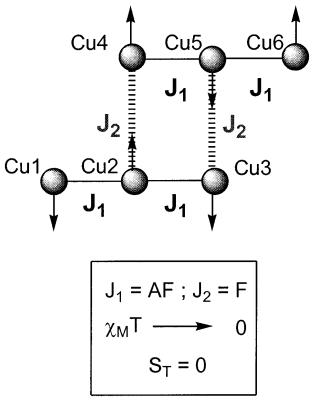

Figure 10. Scheme of the spin topology assuming intermolecular ferromagnetic coupling for a ring of six copper(II) atoms.

K at 2 K. For **3**, the shape of the curve and the $\chi_M T$ values are very similar to those of complex **2**: the $\chi_M T$ value decreases gradually from 2.26 cm^3 mol^{-1} K at 300 K with a plateau between 40 and 15 K (0.95 cm^3 mol^{-1} K), and from 15 to 2 K $\chi_M T$ slightly decreases to 0.90 cm^3 mol^{-1} K. The shape of the curves from room temperature to 15 K is typical of a ferrimagnetic trinuclear Cu^{II} complex.[16a] The decrease of the $\chi_M T$ value in the low-temperature region is indicative of small intermolecular interactions, through hydrogen bonds, as shown in the structural part (Figure 4). The simulation of the two possible cases (ferro- and/or antiferromagnetic intermolecular interactions for a system of 6 atoms) has been reported elsewhere.[14] The case shown in Figure 10 was used to analyze experimental magnetic measurements and for the treatment of data. When the magnetic interaction between these two entities is weakly ferromagnetic, the resulting S_T value tends to zero at low temperatures, and so the $\chi_M T$ curve decreases and tends to zero at these temperatures. The experimental data were fitted according to the following Hamiltonian:

$$H = -J_1(S_1S_2 + S_2S_3 + S_4S_5 + S_5S_6) - J_2(S_2S_4 + S_3S_5)$$

Here J_1 corresponds to the coupling through the oxamato bridge and J_2 to the coupling through the hydrogen bonding between trinuclear entities. The free parameters were J_1, J_2, and g (average). The fit made by the irreducible tensor formalism (ITO), using the CLUMAG program,[21] gave the following results: $J_1 = -125.77$ cm^{-1}, $J_2 = 0.85$ cm^{-1}, $g = 2.16$, and $R = 3.24 \times 10^{-4}$ for complex **2**; $J_1 = -135.50$ cm^{-1}, $J_2 = 0.94$ cm^{-1}, $g = 2.27$, and $R = 6.25 \times 10^{-5}$ for complex **3**.

EPR Spectra. The main features of the powder EPR spectra at various temperatures for compounds **1**−**3** are summarized in Table 5. Clear temperature dependence is observed upon cooling. At room temperature the three EPR spectra are isotropic with g (average) close to 2.10. The bandwidth is very large (1500−2000 G). On decrease of the temperature, **1**−**3** present axial symmetry with $g_{\parallel} > g_{\perp} > 2.00$. **1** also shows hyperfine splitting in the parallel direction ($A_{\parallel} = 75$ G).

The magnetic susceptibility data show that, at liquid nitrogen temperature and at 4 K, the doublet ground state is

Table 5. Main Features of the EPR Spectra of Compounds **1**−**3** at Different Temperatures

compds	room temp	close to liquid-N_2 temp (77 K)		4 K
1	$g = 2.08$ (isotropic, width 1500 G)[a]	(99 K): $g_{\parallel} = 2.18$, $g_{\perp} = 2.06$, $A_z = 75$ G		$g_{\parallel} = 2.18$, $g_{\perp} = 2.06$, $A_z = 75$ G
2	$g = 2.12$ (isotropic, width 2000 G)[a]	(85 K): $g = 2.11$ (isotropic, width 1000 G)	(45 K): $g_{\parallel} = 2.18$, $g_{\perp} = 2.10$	$g_{\parallel} = 2.18$, $g_{\perp} = 2.10$
3	$g = 2.11$ (isotropic, width 1800 G)[a]	(89 K); $g = 2.11$ (isotropic, width 1000 G)	(45 K): $g_{\parallel} = 2.19$, $g_{\perp} = 2.10$	$g_{\parallel} = 2.19$, $g_{\perp} = 2.10$

[a] In the three complexes, the bandwidth strongly decreases with temperature.

the most populated for all compounds (**1**−**3**), the **g** tensor of this doublet ground state being related to the individual tensor of the copper ions by[22]

$$\mathbf{g} = 1/3[2g_{T1} - g_C + 2g_{T2}]$$

Thus, at low temperature, where only the doublet ground state is populated, the **g** tensor of the doublet ground state is expected to be less anisotropic than the **g** tensor of the mononuclear species (in average).

Another effect should be taken into consideration. Even an extremely weak value of intermolecular exchange interactions leads to the exchange averaging effect, which is responsible for the isotropic spectra at room temperature.[16a] It is well-known that exchange averaging conditions are frequently fulfilled for mononuclear copper(II) complexes.[16a] Therefore, it is highly probable that the intermolecular exchange averaging condition is always fulfilled for trinuclear copper(II) complexes.

Therefore, the bands are very broad and isotropic at room temperature, whereas, at lower temperature, the signals become sharp and anisotropic but less pronounced than in most copper(II) mononuclear species with the unpaired electron in an $d_{x^2-y^2}$ orbital.

Discussion

In complex **1**, like in all the complexes reported with oxamato derivatives and tmen as blocking ligand, the Cu^{II} terminal atoms have a 4 + 1 square-pyramid environment, the basal plane are formed by the two nitrogen atoms of the tmen and two oxygen atoms of the oxamato bridge, and the apical position is occupied by a water molecule, counteranions (such as ClO_4^-, PF_6^-), or XCN^- (X = Se, S). The magnetic orbitals are well described by the antibonding combination of the $d_{x^2-y^2}$ metallic orbitals with the symmetry-adapted molecular orbitals of the oxamato bridge, and they lie in the base of the square pyramid as shown in Figure 11a; all *J* values are higher than -330 cm^{-1}. For complexes **2** and **3**, the square pyramidal environment of the terminal copper(II) is strongly modified with an oxygen atom of oxamato bridge occupying the apical position. This change in the square-pyramid environment of the terminal copper(II) ions gives the "orbital reversal" described by Kahn[23] for oxalato complexes. This feature reduces the overlap because the terminal magnetic orbitals are located in planes orthogonal to the oxamato bridge as shown in Figure 11b. These data explain why the *J* values (antiferromagnetic coupling through the oxamato bridge) for complexes **2** and **3** are the lowest reported so far with oxamato ligands and bidentate amines as blocking ligands.

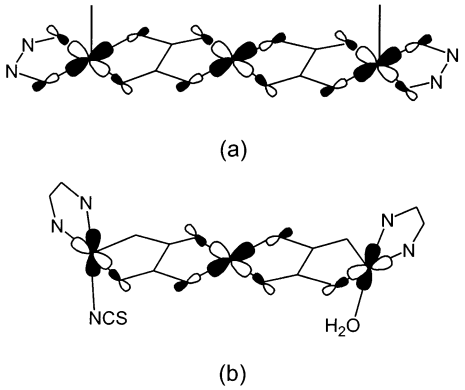

Figure 11. Relative orientations of the magnetic orbitals when they lie (a) all coplanar in square-based pyramidal coordination and (b) in distinct planes with square-based pyramidal coordination for both Cu^{II} terminal ions.

Concerning the intermolecular hydrogen bonds, a few reports have implicated H-bond water pathways in intermolecular ferromagnetic coupling.[24] The small ferromagnetic coupling found in complexes **1**−**3** may be due to the fact that the water molecules that participates in the bond are apical to the square-pyramid Cu^{II} ions, and thus the possible overlap between the magnetic orbitals should be close to zero or even nil, taking into account the orthogonality of these orbitals.

Conclusions

In this study, we have synthesized the complex $[\{Cu(H_2O)(tmen)Cu(NCS)(tmen)\}\{\mu\text{-}Cu(H_2O)(Me_2pba)\}]_2(ClO_4)_2 \cdot 4H_2O$ (**2**) starting from $[\{Cu(H_2O)(tmen)\}_2\{\mu\text{-}Cu(H_2O)(Me_2pba)\}]_2\{(ClO_4)_2\}_2$, previously reported by us.[14] To prepare the analogous complex with PF_6^- (**3**) instead of ClO_4^-, we previously synthesized the $[\{Cu(H_2O)(tmen)Cu(tmen)\}\{\mu\text{-}Cu(H_2O)(Me_2pba)\}]_n\{(PF_6)_2\}_n \cdot 2nH_2O$ compound **1**. The change in the counteranion modifies the self-assembled process between the trinuclear entities: for the complex with ClO_4^- the self-assembled process gives hexanuclear entities, instead of the one-dimensional entities obtained for complex **1** (with PF_6^-). Our main aim was to self-assemble these trinuclear entities through the SCN^- ligand, as reported

(22) Bencini, A.; Gatteschi, D. *EPR of Exchange Coupled Systems*; Springer-Verlag: Berlin, 1990.
(23) Kahn, O. *Molecular Magnetism*; VCH Publishers: New York, 1993; pp 169 and 255.
(24) (a) Scaringe, R. P.; Hatfield, W. E.; Hodgson, D. J. *Inorg. Chem.* **1977**, *16*, 1600. (b) Drijaca, A.; Hockes, D. C. R.; Moubaraki, B.; Murray, K. S.; Spiccia, L. *Inorg. Chem.* **1997**, *36*, 1988.

when the oxamato was 1,3-propanediylbis(oxamato).[15a] Unexpectedly, when this oxamato derivative is replaced by 2,2-dimethyl-1,3-propylenebis(oxamato), the SCN group behaves only as a terminal ligand and the self-assembled process occurs through hydrogen bonds giving hexanuclear entities. In these hexanuclear entities there is a unique feature not previously shown for oxamato bridges and bidentate amine ligands: the apical position in the square-pyramid environment of the terminal Cu^{II} ions is occupied by an oxygen atom of the oxamato skeleton, giving rise to a new type of orbital reversal, which strongly reduces the antiferromagnetic coupling.

Acknowledgment. This study was supported by Grant BQU2000/0791 from the Dirección General de Investigación Científica y Técnica (Spanish Government).

Supporting Information Available: Three X-ray crystallographic files, in CIF format. This material is available free of charge via the Internet at http://pubs.acs.org.

IC011081I